Published in final edited form as:
Biochemistry. 2008 December 2; 47(48): 12860–12868. doi:10.1021/bi801718d.

Cysteine pK_a values for the bacterial peroxiredoxin AhpC[†,‡]

Kimberly J. Nelson[§], **Derek Parsonage**[§], **Andrea Hall**[‖], **P. Andrew Karplus**[‖], and **Leslie B. Poole**[*,§]

§*Department of Biochemistry, Wake Forest University School of Medicine, Winston-Salem, North Carolina 27157*

‖*Department of Biochemistry and Biophysics, Oregon State University, 2011 Ag Life Sciences Building, Corvallis, Oregon 97331*

Abstract

Salmonella typhimurium AhpC is a founding member of the peroxiredoxin family, a ubiquitous group of cysteine-based peroxidases with high reactivity toward hydrogen peroxide, organic hydroperoxides and peroxynitrite. For all of the peroxiredoxins, the catalytic cysteine, referred to as the peroxidatic cysteine (C_P), acts as a nucleophile in attacking the peroxide substrate, forming a cysteine sulfenic acid at the active site. Because thiolates are far stronger nucleophiles than thiol groups, it is generally accepted that cysteine-based peroxidases should exhibit pK_a values lower than an unperturbed value of 8.3 – 8.5. In this investigation, several independent approaches were used to assess the pK_a of the two cysteinyl residues of AhpC. Methods using two different iodoacetamide derivatives yielded unperturbed pK_a values (7.9 – 8.7) for both cysteines, apparently due to reactivity with the "wrong" conformation of C_P (i.e. locally unfolded and flipped out of the active site), as supported by X-ray crystallographic analyses. A functional pK_a of 5.94 ± 0.10 presumably reflecting titration of C_P within the fully folded active site was obtained by measuring AhpC competition with horseradish peroxidase for hydrogen peroxide; this value is quite similar to that obtained by analyzing the pH dependence of the ε_{240} of wild-type AhpC (5.84 ± 0.02), and similar to those obtained for two typical 2-cysteine peroxiredoxins from *Saccharomyces cerevisiae* (5.4 and 6.0). Thus, the pK_a value of AhpC balances the need for a deprotonated thiol (at pH 7, ~90% of the C_P would be deprotonated) with the fact that thiolates with higher pK_a values are stronger nucleophiles.

Keywords

peroxiredoxins; alkyl hydroperoxide reductase; peroxidases; disulfide redox centers; antioxidants; thiolate

[†]This study was supported by a grant from the National Institutes of Health to L.B.P. with a subcontract to P.A.K. (RO1 GM050389), a grant from the National Science Foundation to Jacquelyn S. Fetrow with L.B.P. as a co-investigator (MCB-0517343), and a Ruth L. Kirschstein Individual Fellowship from the National Institutes of Health to K.J.N (F32 GM074537)

[‡]The coordinates and structure factors have been deposited in the Protein Data Bank (PDB) with an ID code of 3EMP.

*To whom correspondence should be addressed (Poole tel. 336-716-6711, fax 336-777-3242), e-mail: lbpoole@wfubmc.edu.

Salmonella typhimurium AhpC (*St*AhpC)[1] is a member of the peroxiredoxin (Prx) family, a ubiquitous group of cysteine based peroxidases with high reactivity toward H_2O_2 [K_m for H_2O_2 of 1.4 μM; k_{cat}/K_m of 4 x 10^7 M^{-1} s^{-1} for *St*AhpC] (1). For all of the Prxs, the catalytic cysteine, referred to as the peroxidatic cysteine (C_P) acts as a nucleophile to attack and reduce the peroxide substrate, and in doing so becomes oxidized to form a cysteine sulfenic acid. The fate of the sulfenic acid differs in various Prx enzymes, forming a disulfide bond either with another cysteine in the Prx, or with an external thiol in redox donors such as thioredoxin, glutaredoxin, or reduced glutathione (2-Cys and 1-Cys Prx mechanisms, respectively). The typical 2-Cys Prxs, which form an intersubunit disulfide bond during turnover, include *St*AhpC and are the most widely distributed and abundant type of Prxs. In mammalian cells they are on the order of 1% of the soluble protein (2,3). AhpC in *Escherichia coli* has been shown to have a primary role as a peroxide scavenger (4), but since the discovery that many eukaryotic Prxs have an evolutionarily selected sensitivity to inactivation by peroxide (5), evidence has been accumulating supporting the hypothesis that the primary role of these enzymes in higher organisms is to regulate peroxide signaling (2,6,7).

Crystal structures of *St*AhpC have shown that the cysteines residues are oriented in very different ways depending upon the redox state of the protein. The structure of *St*AhpC with the C_P mutated to Ser mimics the reduced conformation and represents a fully folded structure with the thiol(ate) form of the C_P (C46) present in the first turn of an α-helix protruding into a highly conserved active site pocket, interacting with conserved Arg and Thr residues that likely serve to enhance its nucleophilicity (5). The C_R (C165) is in the C-terminal end of the protein and is ~13 Å apart from and pointing away from the C_P. In contrast, the structure of the disulfide-bonded protein exhibits a local unfolding of the α-helix containing the C_P, flipping the thiol group out of the active site pocket (8). The C_R is also reoriented in this structure and the C-terminus beyond C165 (21 residues) is disordered. Analysis of the subunit composition of *St*AhpC by analytical ultracentrifugation has shown that there is an intimate link between redox state and oligomeric arrangement for *St*AhpC; the reduced protein is a strong decamer in solution while the oxidized protein tends to dissociate into dimers (8). Recent studies have shown that the decameric arrangement of *St*AhpC enhances the peroxide reductase activity of *St*AhpC, presumably through the stabilization of the fully folded active site by the dimer-dimer interface (1). If the local unfolding is unfavorable, as is the case for some eukaryotic enzymes, then the enzyme is highly sensitive to inactivation via further oxidation of C_P by a second molecule of peroxide, leading to formation of a sulfinic acid (C_P-SO_2H). While *St*AhpC is resistant to inactivation, this pathway appears to be important for peroxide signaling in eukaryotes (5,9).

It is generally accepted that, because thiolates are far stronger nucleophiles than thiol groups, cysteine-based peroxidases should exhibit pK_a values that are significantly lower than the value of 8.3 – 8.5 observed for free cysteine to promote thiolate formation at the active site (10). There is a trade-off with lowering the cysteine pK_a, however, in that the intrinsic nucleophilicity of a thiolate is lowered as the pK_a is decreased (11,12). In spite of the importance of this property for chemical reactivity of Prxs, pK_a values for the C_P in Prxs have been assessed in only a very few cases. The reported values range from pH 6.0 and 5.4 for yeast Tsa1 and Tsa2 (also known as cTPx1 and cTPx2) (13) to <5 reported for *St*AhpC (14), although a rigorous

[1]Abbreviations: Prx, peroxiredoxin; AhpC, alkyl hydroperoxide reductase C component (the cysteine-based peroxidase); *St*AhpC, AhpC from *Salmonella typhimurium*; AhpF, alkyl hydroperoxide reductase F component (the flavoprotein disulfide reductase); C_P, peroxidatic cysteine (C46) of AhpC; C_R, resolving cysteine (C165) of AhpC; HRP, horseradish peroxidase; DTNB, 5,5′-dithiobis(2-nitrobenzoic acid); SDS, sodium dodecyl sulfate; PAGE, polyacrylamide gel electrophoresis; DTT, 1,4-dithiothreitol; GuHCl, guanidine hydrochloride; DTPA, diethylenetriamine pentaacetic acid; EDTA, ethylenediamine tetraacetic acid; IAAn, iodoacetanilide; d_5-IAAn, deuterated iodoacetanilide; d_0-IAAn, protiated iodoacetanilide; MALDI-TOF, matrix-assisted laser desorption/ionization time-of-flight; MS, mass spectrometry; AhpC-C46AAn, S-acetanilide modified form of the C165S mutant of AhpC; MES, 2-(N-morpholino) ethanesulfonic acid.

experimental determination of the pK_a for the active site cysteine has not been carried out for *St*AhpC or most other Prxs. Here we present data from multiple different approaches used to assess the pK_a of the cysteinyl residues of *St*AhpC. The pH dependence of alkylation rates using two different iodoacetamide derivatives yielded unperturbed pK_a values between 7.9 and 8.7 for both cysteines, apparently due to reactivity with the "wrong" conformation of C_P (i.e. flipped out of the active site), as supported by crystallographic analyses. Two other independent methods yielded perturbed pK_a values of about 5.8 and 5.9 for C46 of wild type AhpC. The latter is, in fact, a functional pK_a based on peroxide reactivity, supporting the interpretation that this measured pK_a corresponds to the cysteine thiol(ate) within the active site.

Experimental Procedures

Materials

Horseradish peroxidase, type VI (HRP), NADH, iodoacetamide, trichloroacetic acid, calcium chloride, ammonium sulfate, sodium citrate, boric acid, and sodium phosphate were purchased from Sigma. 5-Iodoacetamidofluorescein was purchased from Molecular Probes (Invitrogen). TPCK-treated trypsin was from Worthington Biochemicals, and 1,4-dithiothreitol (DTT) was from Anatrace. Diethylenetriamine pentaacetic acid (DTPA) and 2,5-dihydroxybenzoic acid were purchased from Acros Organics. Guanidine hydrochloride (GuHCl) was from Lancaster Synthesis (Ward Hill, MA). Ethylenediamine tetraacetic acid (EDTA), 2-mercaptoethanol, ammonium bicarbonate, and 5,5′-dithiobis(2-nitrobenzoic acid) (DTNB) were purchased from Research Organics. Sodium citrate, HCl, acetonitrile, and hydrogen peroxide were from Fisher, and PD-10 desalting columns were from GE Healthcare. Deuterated (d_5) and protiated (d_0) N-phenyl iodoacetamide (iodoacetanilide, abbreviated d_5-IAAn and d_0-IAAn, respectively) were synthesized as described previously (15).

Methods

Protein Expression and Purification—Wild type *Salmonella typhimurium* AhpC and two mutant forms, C46S and C165S, were expressed in a non-His-tagged form from a vector, pTHCm-*ahpC*, derived from Invitrogen's pTrcHisA in which the *beta*-lactamase gene was replaced by a chloramphenicol resistance gene. *E. coli* strain TA4315 (16) was used for expression of all AhpC proteins. The purification procedure for all proteins was essentially the same as described previously (17,18); DTT was maintained at 5 mM in all buffers used during the purification of C165S in order to prevent hyperoxidation of the C_P. AhpC concentrations (in terms of monomers) were determined by absorbance at 280 nm with $\varepsilon = 24{,}300\ M^{-1}\ cm^{-1}$ (17).

Stability of AhpC Toward Denaturation By GuHCl or Prolonged Incubation in Various pH Buffers—AhpC (20 μg) in 1.5 mL of buffer containing 10 mM sodium phosphate, 10 mM boric acid, 10 mM sodium citrate, 1 mM EDTA, and 100 mM ammonium sulfate (pH 7.0) including varying concentrations of GuHCl (0-6 M) at 25 °C was incubated for 2 h followed by measurement of the intrinsic tryptophan fluorescence at λ_{ex} = 280 nm and λ_{em} = 350 nm using an Aminco-Bowman Series 2 luminescence spectrofluorometer. The photomultiplier tube voltage was set so that a fresh sample without GuHCl gave a fluorescence intensity that was 50% of the maximal fluorescence value.

To assess structural stability of the native protein in various pH buffers, AhpC (20 μg) was incubated at 23 °C for 24 h in a final volume of 1.5 mL at various pH values from 3 to 10 in a buffer containing 10 mM sodium phosphate, 10 mM sodium citrate, 10 mM boric acid, 1 mM EDTA, and 100 mM ammonium sulfate (BPACE buffer), with the pH adjusted with either ammonium hydroxide or sulfuric acid. The intrinsic tryptophan fluorescence for each sample was measured as described above. After recording the data at each pH, the fluorescence

intensity for each sample was measured under denaturing conditions by the addition of 10 μL concentrated HCl.

Analysis of pK_a Using pH Dependence of 240 nm Absorbance—AhpC (wild type and mutants) was reduced with 10 mM DTT for 10 min at room temperature, then separated from the DTT using a PD-10 size exclusion column. The absorbance of 3 to 10 μM protein was measured in 1X BPACE buffer on an Agilent HP8453 diode array spectrophotometer at a variety of pH values. The amount of protein in solution was determined spectrophotometrically at 280 nm as described above and used to calculate the ε_{240} at each pH. This value was plotted against pH and the pK_a was determined by direct fit to equation 1,

$$y = \left[\left(A \times 10^{pH}\right) + \left(B \times 10^{pKa}\right)\right] / \left(10^{pKa} + 10^{pH}\right) \quad (1)$$

where y = ε_{240}, A = the upper plateau at high pH (ε_{240} for the deprotonated form), and B = the lower plateau at low pH (ε_{240} for the protonated form).

Determination of Cysteine pK_a By Reactivity With Fluorescein Iodoacetamide Across a Range of pH Values—Wild type AhpC was reduced and reisolated from the DTT as described above. The protein was diluted to a final concentration of 0.5 mg/mL (24.3 μM) in 1X BPACE buffer at various pH values and incubated with 180 μM fluorescein iodoacetamide; after various incubation times, 20 μL aliquots were removed and quenched with 10 μL of 600 mM 2-mercaptoethanol. Samples were then separated by 12% SDS-PAGE, and the fluorescence associated with the protein and with the dye front (unreacted reagent) was measured on a STORM 840 fluorescence imager. Fluorescence intensity was determined using ImageQuant 5.2 gel analysis software. The percent of fluorescence in the protein fraction was plotted against time and fit to a single exponential equation to determine the k_{obs}. The k_{obs} at each pH was then plotted against pH and the pK_a was determined by direct fit to equation 1, where y = k_{obs}, A = the upper plateau at high pH (the rate of reaction of the deprotonated form), and B = the lower plateau at low pH (the rate of reaction of the protonated form).

Determination of Cysteine pK_a By Reactivity With Iodoacetanilide (IAAn) Across a Range of pH Values Using Isotope Coded Reagents and MALDI-TOF Mass Spectrometry Analyses—As an internal standard for quantitation, reduced AhpC was incubated with a 5-fold excess of d_5-IAAn at 24 °C for 21 h. After confirming complete reaction by MALDI-TOF MS, the resulting protein was exchanged into 25 mM ammonium bicarbonate at pH 8.5 and stored at -20 °C until needed.

AhpC (0.5 mM) was reduced with 10 mM DTT for 10-15 min, then reisolated using a PD10 column. The reaction mixture was prepared with a final concentration of 40 μM AhpC in a total volume of 1.055 mL using 1X BPACE buffer at the desired pH. The reaction was initiated by the addition of 400 μM (final concentration) d_0-IAAn, and aliquots of 2.5 nmol AhpC were removed at appropriate time points and quenched with 500 mM 2-mercaptoethanol. A standard amount of AhpC labeled with d_5-IAAn (1.25 nmol) was added to each sample prior to precipitation on ice with cold trichloroacetic acid at 10% final concentration. After centrifugation, the protein pellet was washed with 0.5 mL of 1:1 ether:ethanol, recentrifuged and resuspended in 40 mM ammonium bicarbonate, 1 mM $CaCl_2$, and 10% acetonitrile at pH 8.5 and digested overnight at 37 °C with 2.5 ng (50 ng/mL) trypsin. The two cysteines of AhpC are located on different tryptic peptides; C46 was monitored at 3836 or 3841 Da (representing the d_0- and d_5-labeled peptides, respectively; WSVFFFYPADFTFVCPTELGDVADHYEELQK), and C165 was monitored at 1745 or 1750 Da (representing the d_0- and d_5-labeled peptides, respectively; AAQYVAAHPGEVCPAK) on

a Brüker Autoflex MALDI-TOF mass spectrometer using dihydroxybenzoic acid as the matrix. Data were collected three times for every sample using the Autorun feature on the instrument. Peak intensities were used to determine the ratio of light to heavy peptides, and the ratios were plotted against time and fit to a single exponential equation to determine k_{obs}. The actual pH of each reaction mixture was measured for the remaining sample. The k_{obs} at each pH was plotted against pH and the pK_a was determined by direct fit to equation 1.

Determination of Reaction Rates of AhpC With Iodoacetamide, Fluorescein Iodoacetamide and IAAn at pH 7—Wild type AhpC was reduced and exchanged into BPACE pH 7.0 as described above. AhpC was diluted to 40 μM and the reaction was initiated by the addition of iodoacetamide, fluorescein iodoacetamide or IAAn. For fluorescein iodoacetamide modification, the reaction progress was monitored by fluorescence after SDS-PAGE as described above. To measure reaction progress with iodoacetamide or IAAn, an aliquot of each sample at various times was quenched by addition of 100 mM DTT, then applied to a Bio-Gel P6 spin column to remove small molecules and exchange the protein into 25 mM potassium phosphate buffer with 1 mM EDTA, pH 7.2. The loss of free thiol groups was monitored by addition of 0.25 mM DTNB (final concentration) to a cuvette containing 170 μL of the spin column flowthrough and 360 μL of buffer, and measurement of the 412 nm absorbance. The concentration of free thiols was then determined based on the release of 2-nitro-5-thiobenzoate (ε_{412} = 14,150 M^{-1} cm^{-1}) (19). Protein concentration was determined by measurement of the 280 nm absorbance before DTNB addition.

Crystal Structure Determination of the IAAn Adduct of C165S AhpC—Purified C165S AhpC was separated from the DTT in the storage buffer using a PD10 column, then incubated with a 4-fold excess of d_0-IAAn for 17 h at 4 °C in 25 mM phosphate, 1 mM EDTA, pH 7.0. MALDI-TOF MS analysis confirmed that the protein was completely alkylated. The protein was then exchanged into 25 mM phosphate, 1 mM EDTA (pH 7) using a G25 size exclusion column to remove excess reagent and concentrated to 14.6 mg/mL using 20 kDa cutoff Apollo ultrafiltration devices (Orbital Biosciences, Topsfield, MA).

Crystals of the S-acetanilide modified form of C165S (AhpC-C46AAn) were grown at 4 °C in hanging drops using a 0.4 mL reservoir solution with drops containing a 2:1 ratio of protein stock solution to reservoir solution. Commercial Wizard II screen condition #45 [Emerald Biosystems, 1.26 M $(NH_4)_2SO_4$, 0.1 M 2-(N-morpholino)ethanesulfonic acid (MES) pH 6.0] produced the best crystals. The rectangular prism crystals appeared after two weeks, growing out of a precipitate to a final size of 0.25 x 0.25 x 0.1 mm^3. Crystals were harvested into 1.2 M $(NH_4)_2SO_4$, 0.1 M MES, pH 6.0, and for data collection, crystals were placed in the same buffer plus 25% glycerol for 1 min, mounted in loops and flash frozen in liquid nitrogen.

Oscillation data were collected in house using Cu-Kα radiation, an R-axis IV detector and Δφ = 1.0°. The crystals belong to trigonal space group $P3_121$ with one half-decamer in the asymmetric unit and unit cell dimensions a = b = 136.91 Å, c = 145.42 Å. AhpC-C46AAn data were merged from two isomorphous crystals, one with 60 images (20 min/image) and the other with 90 images (30 min/image). Useable data extended to 4.0 Å resolution (Table 1).

All crystallographic calculations were performed using ccp4 (20) version 5.99.5 and model viewing was done using Coot (21) version 0.2. The structure of AhpC-C46AAn was determined by molecular replacement using AmoRe (22). Two search models were used, an AhpC structure with a fully folded active site (PDB entry 1N8J) and an AhpC structure with a locally unfolded active site (the T77V mutant of AhpC, PDB entry 1YF1). For the search models, only the protein atoms for one half-decamer (chains A-E) were used. For the fully folded model, all chains were truncated after residue 166; for the locally unfolded model no chains extended beyond residue 165 so no truncation was needed. Five percent of the data were randomly

selected for cross-validation. Using data from 15 to 4 Å resolution, both search models gave a unique solution that packed well in the unit cell. After rigid body refinement, no additional refinement was carried out before selection of the correct model due to the low resolution of the data. Electron density maps were calculated from both the fully folded and locally unfolded models. Omit maps were also generated from both models by removing residues 41 through 48 from each subunit prior to rigid body refinement. Non-crystallographic symmetry averaging was performed using DM (23) to improve the signal to noise ratio for each of the four maps. The locally unfolded model was further refined as a rigid body after removing significant clashes in the model by truncating all chains at residue 162 and using the "rigid body fit zone" option of Coot (18) to shift segments 28-31, 56-64, 125-129, 136-140, and 148-162 of chain A. The final model had R/Rfree=0.301/0.308 and has been deposited in the Protein Data Bank with pdb code 3EMP.

Determination of Functional pK_a By pH-Dependence of Competition With HRP For Hydrogen Peroxide—The pH dependence of the AhpC reaction with H_2O_2 was determined by monitoring the ability of AhpC to compete with HRP based on the method of Ogusucu et al. (13). Briefly, HRP was dissolved in 5 mM potassium phosphate buffer with 0.1 mM DTPA, pH 7.0, and the concentration of the HRP stock was determined by measuring the absorbance at 403 nm ($\varepsilon_{403} = 1.02 \times 10^5\ M^{-1}\ cm^{-1}$) (24,25). Wild-type AhpC was reduced with 10 mM DTT for 1 h at room temperature, then separated from the DTT using a PD-10 column and exchanged into 5 mM phosphate buffer containing 0.1 mM DTPA at pH 7.0. Stock solutions containing HRP and AhpC in the same buffer (75 μL) were aliquoted into a 96 well microplate, then mixed with 1 volume of buffer at various pH values between 4 and 9.5 to give a

$$\left(\frac{F}{1-F}\right) k_{HRP}\ [HRP] = k_{AhpC}\ [AhpC] \tag{2}$$

final concentration of 10 mM phosphate, 10 mM boric acid, 10 mM sodium citrate, 100 mM sodium chloride, 0.1 mM DTPA, 7.5 μM HRP, and 0, 2, 4, 8, 12, or 16 μM AhpC in a final volume of 150 μL. The starting HRP absorbance for each sample was determined at 403 nm in a Tecan Safire 2 microplate reader. The reaction was started by the addition of 10 μL of 45 μM H_2O_2 in deionized H_2O (final concentration of H_2O_2 = 3 μM). The extent of HRP oxidation by H_2O_2 was determined by monitoring the change in absorbance at 403 nm within 90 s of peroxide addition. The actual pH was determined by making a 1:1 dilution of each pH buffer into 5 mM phosphate containing 0.1 mM DTPA, mimicking the reaction mixtures. The percentage of inhibition of HRP oxidation (F/1–F) at each AhpC concentration (see Supplemental Information for details) was plotted against [AhpC] in order to obtain the second-order rate constant for AhpC (k_{AhpC}) as established by equation 2 (26). Above pH 5, a second order rate constant of $1.8 \times 10^7\ M^{-1}\ s^{-1}$ (24) for k_{HRP} was used. Below pH 5, the second order rate constant for HRP was calculated for each pH using equation 3 and the ionization constants determined in the previous study (24) ($K_1 = 5.64 \times 10^{-4}$ and $K_2 = 1.29 \times 10^{-4}$):

$$k_{HPR} = \left(1.78 \times 10^7\ M^{-1}\ s^{-1}\right) / \left(1 + [H^+]/K_2 + [H^+]/K_1K_2\right) \tag{3}$$

The k_{AhpC} at each pH was plotted *versus* pH and the pK_a was calculated by direct fit to equation 1, where $y = k_{AhpC}$.

Results

Stability of StAhpC After Prolonged Incubation in Buffers at Various pH Values

Changes in protein conformation often result in alterations in the fluorescence properties of a protein due to changes in the local environment of the tryptophan residues. AhpC has three tryptophan residues (W32, W81 and W169), with one, W81, located near C46. While no difference can be observed in the fluorescence properties of reduced and oxidized AhpC, protein denaturation in the presence of 3 M GuHCl or 80 mM HCl results in a 70% decrease in the fluorescence intensity of AhpC with excitation at 280 nm and emission at 350 nm (see Supplemental Information, Figure S1). Because this serves as a sensitive probe of the folding status of this protein, AhpC fluorescence was measured after 24 h incubations in buffers between pH 3 and 11. No significant change was observed in the fluorescence intensity of either reduced or oxidized AhpC between pH 4.5 and 10, indicating that both are stable across the pH range required for pK_a determinations. In further experiments, AhpC fluorescence did not change over 20-30 min in buffers at pH values down to 4.14, allowing relatively short experiments to be conducted without stability problems within this limited range.

Determination of Cysteine pK_a By Measuring Absorbance at 240 nm Across a Range of pH Values

Absorbance at 240 nm has been used previously to monitor the protonation state of cysteine residues in proteins (27-29). Given the stability results described above, the ε_{240} was determined for both oxidized and reduced wild-type AhpC at a variety of pH values between 4.5 and 9.5. While the oxidized protein did not exhibit a significant pH-dependent change in ε_{240}, the reduced protein exhibited a single apparent pK_a value of 5.84 ± 0.02 (Figure 1a). The difference in ε_{240} between reduced AhpC at high pH and the oxidized protein was ~9,700 M^{-1} cm^{-1}. If a standard range of ε_{240} for a single thiol group of 4,000 – 6,000 M^{-1} cm^{-1} (27) were used, this would suggest that two cysteine residues with similar pK_a values were undergoing changes in protonation state during the course of this titration. This interpretation is not clearcut, however, since thiolate extinction coefficients may be quite variable, with reported values as low 2,300 and as high (at 229 nm) as 7,500 M^{-1} cm^{-1} (30,31). Furthermore, the presence of nearby aromatic residues may alter the spectral signature of this ionization. Given data presented below, we can be relatively confident that C46 is centrally involved in the extinction coefficient change observed at 240 nm; whether or not C165 also titrates through this pH range with a very similar pK_a is not clear.

In order to distinguish the pK_a values for each individual cysteine and provide for an additional control titration in an AhpC lacking both cysteine residues, the experiment was repeated using the single cysteine mutants, C165S and C46S, and the double cysteine mutant C46S/C165S. Not surprisingly, the C165S/C46S mutant did not exhibit a significant pH-dependent change in the ε_{240} (Figure 1b). While there were some pH-dependent changes observed in ε_{240} for both the C165S and C46S mutants (Figure 1b), these changes were neither large enough nor in the expected direction to permit an evaluation of the cysteine pK_a values, nor did they help in the interpretation of the pK_a value obtained for the titration of the wild type protein. These complexities suggested that this type of analysis for AhpC may be confounded by additional conformational changes occurring during the pH titration, at least in the case of the mutant proteins.

Determination of Apparent Cysteine pK_a By Monitoring Reactivity With Iodoacetamide Derivatives Across a Range of pH Values

Although a reasonable pK_a value was obtained for the wild type protein by monitoring the ε_{240}, the single apparent pK_a value obtained for the two cysteine residues in wild type AhpC and the inconsistencies with the mutant proteins made it imperative to evaluate the pK_a values

using alternative methods. Nuclear magnetic resonance approaches, which in favorable cases also allow monitoring of the protonation/deprotonation behavior of cysteine residues in their native environment across a pH range, did not turn out to work for this protein. Even when 2-^{13}C-cysteine was incorporated, neither cysteine signal was readily distinguished by ^{13}C NMR; this is not surprising since the decameric form of AhpC is very large and would result in a significant broadening of peaks due to slow tumbling of the protein in solution (K. J. Nelson, D. A. Horita and L. B. Poole, unpublished results).

Because the protonated form of cysteine is unreactive with iodoacetamide, the increase in reaction rate with this reagent as pH increases reflects titration of the target cysteine residue (in the absence of changes in environment and/or accessibility of the target cysteine residue), and this technique has frequently been used to determine cysteine pK_a values (32-35). In order to obtain the pK_a value for both the peroxidatic (C46) and resolving (C165) cysteines, fluorescein iodoacetamide was incubated with either the C165S or C46S mutant of AhpC, and the rate of alkylation was determined by measuring the fluorescence intensity associated with the protein band after SDS-PAGE (Fig. 2a). Using this technique, the pK_a values for C46 and C165 were 7.87 ± 0.06 and 8.64 ± 0.05, respectively. Both of these values are much higher than the value determined for wild type AhpC by measuring the pH dependence of ε_{240} and are approaching the pK_a value of 8.44 measured for free cysteine (10), suggesting that fluorescein iodoacetamide might be reacting with both cysteine residues of AhpC in the locally unfolded rather than fully folded conformation.

A new isotope-coded method was recently developed in our laboratory to determine cysteine pK_a values by monitoring the pH dependence of their reactivity with IAAn (15). The rate of reaction with the protiated version of this reagent (d_0-IAAn) was determined using mass spectrometry to compare the intensity of the alkylated tryptic peptide to a standard amount of the same peptide labeled with the deuterated version of the reagent (d_5-IAAn). This method was tested with *E. coli* thioredoxin and gave pK_a values very similar to those previously published for chemical modification studies with this protein (15). This technique can be used to study wild type AhpC directly since both cysteine residues in this protein are on different tryptic peptides. As cumene hydroperoxide is similar in size and a reasonably good substrate for AhpC (36), IAAn, which also possesses a phenyl group, could be expected to access the active site pocket as a substrate analogue during modification of the protein. Using this technique, the pK_a values obtained for C46 and C165 were similar to those obtained with fluorescein iodoacetamide, however, at 8.55 ± 0.21 and 8.74 ± 0.19, respectively (Figure 2b).

We previously showed that IAAn is about 3-fold more reactive with free cysteine than is iodoacetamide (15). Interestingly, AhpC reacted 8.9-fold more rapidly with IAAn than with iodoacetamide at pH 7, suggestive of an activating effect from the hydrophobic nature of the IAAn (Table 2). The reaction rates of fluorescein iodoacetamide, IAAn, and the smallest of the reagents, iodoacetamide, are relatively slow compared to turnover rates of about 3100 min^{-1} and 2400 min^{-1} with hydrogen peroxide and cumene hydroperoxide, respectively, at 400 μM. In addition, the reactions with both iodoacetamide and IAAn were slower than with fluorescein iodoacetamide, the bulkiest derivative which was expected to have difficulties accessing C46 within the fully folded active site of AhpC. These data along with the fact that the pK_a values were so similar to free cysteine suggested that the peroxidatic cysteine was partially or totally inaccessible within the fully folded protein and that the predominant reaction of these alkylating agents was with the portion of the AhpC population that was in the locally unfolded conformation.

X-Ray Crystal Structure of the IAAn-Generated Adduct of AhpC Confirms a Locally Unfolded Active Site

To determine the conformation of the alkylated AhpC product (AhpC-C46AAn), the crystal structure was obtained for C165S AhpC that had been fully modified with IAAn. Since the usable data only extended to 4.0 Å resolution, search models were used of both a fully folded and a locally unfolded active site in order to compare and control for possible model bias in the electron density maps. For the fully folded structure, the extra step was taken to remove the C-terminal residues from the search model so that any electron density showing up for the ordered C-terminal helix would provide unbiased and strong proof of both its presence and a fully folded active site. Finally, for model selection, model bias was minimized by only carrying out rigid body refinement, and the close match between R and R_{free} values (Table 1) confirms that minimal overfitting has occurred.

The omit maps generated with the fully folded and locally unfolded models show similar electron density in the alkylated AhpC active site and both omit maps clearly follow the path of the locally unfolded model (Figures 3b and 3d). Even if omit maps are not used, the electron density still strongly follows the path of the locally unfolded conformation (Figures 3a and 3c); however, in the map generated using the fully folded model, a slight bias can be seen as the electron density is somewhat stronger along the path of the fully folded chain (Figure 3a). Thus, the active site density is strongly indicative of the structure of AhpC-C46AAn adopting the locally unfolded conformation. Furthermore, independent confirmation that the structure is locally unfolded is provided by the lack of electron density for the C-terminal helix in any of the maps. These results support our hypothesis that these bulky reagents are excluded from the active site and react with the C_P only in its locally unfolded conformation.

Determination of a Functional pK_a For AhpC By Monitoring the pH Dependence of Competition With HRP For Hydrogen Peroxide

In order to directly target AhpC in the fully folded conformation which represents the peroxide-reactive structure, we turned to a technique by which we could monitor the pH dependence of the reaction of AhpC with hydrogen peroxide. The typical activity assay, which includes AhpF or a truncated form of this electron-donating protein (1,17,37), was not used due to potential complications resulting from pH-dependent changes in that protein. Instead, in the experiments undertaken here, the pH dependence of AhpC reduction of H_2O_2 was determined by monitoring the ability of AhpC to compete with HRP in a manner similar to the method used by Ogusucu et al. (13). At pH values of 5 or above, HRP reacts with hydrogen peroxide to produce compound I with a second order rate constant of $1.8 \times 10^7\ M^{-1}\ s^{-1}$ (24), a rate which is nearly identical with that for AhpC with hydrogen peroxide ($3.7 \times 10^7\ M^{-1}\ s^{-1}$). As compound I forms, the 403 nm absorbance of HRP decreases ($\Delta\varepsilon_{403} = 5.4 \times 10^4\ M^{-1}\ s^{-1}$), allowing the amount of HRP oxidation to be determined spectroscopically. The rate of HRP reaction with hydrogen peroxide is independent of pH from 5 to 9.4 as confirmed again in our experiments (see below), which means any difference in rate as a function of pH is due to changes in AhpC reactivity (25). As long as the peroxide concentration is lower than the HRP concentration, the second order rate constant for AhpC reduction of hydrogen peroxide can be determined by plotting the percent inhibition of compound I formation (F/1-F) as a function of AhpC concentration using equation 2.

To test this approach, the amount of HRP (starting concentration = 7.5 μM) oxidized by 3 μM H_2O_2 at pH 7 was monitored in the presence of increasing concentrations of AhpC (0 - 16 μM) (Fig. S2a in Supplemental Information). AhpC inhibited the HRP reaction in a concentration dependent manner and the plot of $(F/1\text{-}F)k_{HRP}[HRP]$ *versus* [AhpC] was linear (Fig. S2b). At pH 7, the second order rate constant obtained using this technique was $3.2 \times 10^7\ M^{-1}\ s^{-1}$. This value is nearly identical to the published value for k_{cat}/K_m of $3.7 \times 10^7\ M^{-1}$

s^{-1} (1), confirming that we are measuring the reaction of AhpC with hydrogen peroxide. The rate of HRP oxidation was also determined in the absence of AhpC by stopped-flow spectroscopy and no change was observed in the rate of compound I formation between pH 5.43 and 9.05 (data not shown). Below pH 5, the rate decreased, consistent with the earlier report by Dolman et al. (24). We therefore corrected the k_{AhpC} at pH 5 and below based on the decreased k_{HRP} calculated from equation 3 and the pK_a values reported earlier (24). The second order rate constants for AhpC reduction of H_2O_2 were determined at various pH values between 4 and 9, and the resulting rates were plotted *versus* pH to obtain a pK_a value of 5.94 ± 0.10 (Figure 4). Because we are measuring the pH dependence of the catalytic activity of the protein, we attribute this pK_a to C46 and can be confident that we are only measuring the conformational state of the protein in which the C_P is activated for peroxide attack (the fully folded conformation).

Discussion

We report here a cysteine pK_a value of 5.84 from ε_{240} measurements and a functional pK_a of 5.94 that is based on reactivity with peroxide. Although the assignment of the spectroscopically determined pK_a to one or both cysteine residues is problematic, the pK_a from the peroxidase rate likely reflects only the protonation state of C46 in the fully folded, active conformation of the protein. Because the locally unfolded form would be essentially unreactive with peroxide at all pH values tested, this species would not be detected in the peroxide competition assay.

The functional pK_a value we observe for AhpC (5.94 ± 0.10) is similar to the values reported by Ogusucu *et al.* for yeast Tsa1 and Tsa2 (5.4 and 6.0) (13) and the estimated pK_a value of 5 to 6 for Prx2 suggested by Peskin *et al.* based upon the relative amount of disulfide bond formation across a range of pH values (38). It is also close to the value obtained by pH dependence of the ε_{240} of AhpC (5.84 ± 0.02), although the behavior of the corresponding mutant enzymes, and particularly C165S, does not firmly support assignment of this pK_a to one or both cysteine residues. Our pK_a values do not agree with an earlier report that suggests that the pK_a for C46 in *St*AhpC is less than 5 (14). Given the difficulties we encountered using alkylating agents in the present study, the slow reaction of iodoacetamide with AhpC, and the use of mutant proteins and a single time point for generating the data in the previous study, our value of 5.9 using the HRP competition assay with wild type AhpC is a more reliable measurement.

The pK_a value for AhpC is not as low as reported for some other proteins that use thiolates in nucleophilic redox reactions such as *E. coli* glutaredoxin-3 (pK_a < 5.5) (39) and DsbA (pK_a = 3.5) (34), but it is lower than the pK_a for the nucleophilic cysteine (C32) of thioredoxin, which is 6.7 – 7.1 (35,40). In fact, a pK_a lower than 5.9 is unlikely to dramatically increase the efficiency of AhpC since a pK_a of 6 means that 91% of the C_P are deprotonated at pH 7 (based upon the Henderson-Hasselbach equation), compared to only 3% of cysteine being deprotonated with a pK_a of 8.5. Also, once the thiolate is formed, its nucleophilicity actually decreases as its pK_a is lowered (11,12), a point that is often missed in the current “reactive cysteine” literature. Given the pK_a of about 5.9, AhpC appears to balance these two factors which affect its enzymatic function.

Alkylation-based studies gave pK_a values around 8.5 for both cysteine residues; the similarity to values for unperturbed free cysteines can be explained by the use of relatively bulky reagents that presumably are excluded from the fully folded active site pocket containing C46, and from the similarly buried C165. Localized unfolding in the region of these residues is well documented (41), and the dynamic effects which allow for transient accessibility of the cysteine residues may be responsible for the relatively slow alkylation observed (Table 2). This was further investigated by X-ray crystallography which indeed showed a locally unfolded

conformation for the IAAn-modified protein. These results therefore support the idea that the reduced enzyme exists in dynamically fluctuating conformations in solution even without prior oxidation of the C_P to sulfenic acid.

We were not able to obtain a clear pK_a value for the C_R in these studies. It is possible that the values of 8.6 – 8.7 obtained from the iodoacetamide-based alkylation experiments are correct for C165 in the fully folded conformation, but we expect from the crystal structure and data with C46 that these values also reflect the locally unfolded conformation of the C_R. Previous studies by Bryk *et al*. using alkylation data also suggested a value of 8.7 for the pK_a of C165 from *St*AhpC (14), but these results may similarly have reflected the locally unfolded rather than fully folded form of C46S.

With the present investigation, the pK_a value for the C_P of *St*AhpC joins those from two other studies of Prxs (13,38) which suggest that the conserved active site environment of this broad family of peroxidases serves to lower the pK_a of the critical cysteine by roughly 2.5 to 3 pH units to a value between 5.4 and 6. Such a pK_a value allows for the C_P within a large percentage of enzyme molecules to exist in its activated, deprotonated state at pH values of 7 or greater, yet helps promote the nucleophilicity of the C_P thiolate which would suffer if the pK_a were lowered even further.

Supplementary Material

Refer to Web version on PubMed Central for supplementary material.

Acknowledgements

The authors thank Amanda Day for technical assistance, Bu-Bing Zeng and S. Bruce King for providing the d_5-IAAn and d_0-IAAn used in these studies, and Dave Horita and Marcus Wright for advice and assistance in acquisition of NMR data for [2-^{13}C]-cysteine labeled AhpC.

References

1. Parsonage D, Youngblood DS, Sarma GN, Wood ZA, Karplus PA, Poole LB. Analysis of the link between enzymatic activity and oligomeric state in AhpC, a bacterial peroxiredoxin. Biochemistry 2005;44:10583–10592. [PubMed: 16060667]
2. Veal EA, Day AM, Morgan BA. Hydrogen peroxide sensing and signaling. Mol Cell 2007;26:1–14. [PubMed: 17434122]
3. Wood ZA, Schröder E, Harris JR, Poole LB. Structure, mechanism and regulation of peroxiredoxins. Trends Biochem Sci 2003;28:32–40. [PubMed: 12517450]
4. Seaver LC, Imlay JA. Alkyl hydroperoxide reductase is the primary scavenger of endogenous hydrogen peroxide in *Escherichia coli*. J Bacteriol 2001;183:7173–7181. [PubMed: 11717276]
5. Wood ZA, Poole LB, Karplus PA. Peroxiredoxin evolution and the regulation of hydrogen peroxide signaling. Science 2003;300:650–653. [PubMed: 12714747]
6. Poole LB, Karplus PA, Claiborne A. Protein sulfenic acids in redox signaling. Annu Rev Pharmacol Toxicol 2004;44:325–347. [PubMed: 14744249]
7. Rhee SG. Cell signaling H_2O_2, a necessary evil for cell signaling. Science 2006;312:1882–1883. [PubMed: 16809515]
8. Wood ZA, Poole LB, Hantgan RR, Karplus PA. Dimers to doughnuts: redox-sensitive oligomerization of 2-cysteine peroxiredoxins. Biochemistry 2002;41:5493–5504. [PubMed: 11969410]
9. Georgiou G, Masip L. An overoxidation journey with a return ticket. Science 2003;300:592–594. [PubMed: 12714731]
10. Luo D, Smith SW, Anderson BD. Kinetics and mechanism of the reaction of cysteine and hydrogen peroxide in aqueous solution. Journal of pharmaceutical sciences 2005;94:304–316. [PubMed: 15570599]

11. Wilson JM, Bayer RJ, Hupe DJ. Structure-Reactivity Correlations for the Thiol-Disulfide Interchange Reaction. J Am Chem Soc 1977;99:7922–7926.
12. Whitesides GM, Liburn JE, Szajewski RP. Rates of thiol-disulfide interchange reactions between mono- and dithiols and Ellman's reagent. J Org Chem 1977;42:332–338.
13. Ogusucu R, Rettori D, Munhoz DC, Soares Netto LE, Augusto O. Reactions of yeast thioredoxin peroxidases I and II with hydrogen peroxide and peroxynitrite: Rate constants by competitive kinetics. Free Radic Biol Med 2007;42:326–334. [PubMed: 17210445]
14. Bryk R, Griffin P, Nathan C. Peroxynitrite reductase activity of bacterial peroxiredoxins. Nature 2000;407:211–215. [PubMed: 11001062]
15. Nelson KJ, Day AE, Zeng BB, King SB, Poole LB. Isotope-coded, iodoacetamide-based reagent to determine individual cysteine pK(a) values by matrix-assisted laser desorption/ionization time-of-flight mass spectrometry. Anal Biochem 2008;375:187–195. [PubMed: 18162165]
16. Storz G, Jacobson FS, Tartaglia LA, Morgan RW, Silveira LA, Ames BN. An alkyl hydroperoxide reductase induced by oxidative stress in *Salmonella typhimurium* and *Escherichia coli*: genetic characterization and cloning of *ahp*. J Bacteriol 1989;171:2049–2055. [PubMed: 2649484]
17. Poole LB, Ellis HR. Flavin-dependent alkyl hydroperoxide reductase from *Salmonella typhimurium*. 1. Purification and enzymatic activities of overexpressed AhpF and AhpC proteins. Biochemistry 1996;35:56–64. [PubMed: 8555198]
18. Ellis HR, Poole LB. Roles for the two cysteine residues of AhpC in catalysis of peroxide reduction by alkyl hydroperoxide reductase from *Salmonella typhimurium*. Biochemistry 1997;36:13349–13356. [PubMed: 9341227]
19. Riddles PW, Blakeley RL, Zerner B. Ellman's reagent: 5,5′-dithiobis(2-nitrobenzoic acid)--a reexamination. Anal Biochem 1979;94:75–81. [PubMed: 37780]
20. The CCP4 suite: programs for protein crystallography. Acta Crystallogr D Biol Crystallogr 1994;50:760–763. [PubMed: 15299374]
21. Emsley P, Cowtan K. Coot: model-building tools for molecular graphics. Acta Crystallogr D Biol Crystallogr 2004;60:2126–2132. [PubMed: 15572765]
22. Navaza J. Acta Crystallogr 1994;A50:157–163.
23. Cowtan K. Joint CCP4 and ESF-EACBM Newsletter on Protein Crystallography 1994;31:34–38.
24. Dolman D, Newell GA, Thurlow MD, Dunford HB. A kinetic study of the reaction of horseradish peroxidase with hydrogen peroxide. Can J Biochem 1975;53:495–501. [PubMed: 237615]
25. Dunford, HB. Spectroscopy of horseradish peroxidase. I. Optical, resonance raman, magnetic circular dichroism, x-ray absorption, and diffraction. In: Dunford, HB., editor. Heme peroxidases. Wiley; New York: 1999. p. 135-174.
26. Winterbourn CC. The ability of scavengers to distinguish OH production in the iron-catalyzed Haber-Weiss reaction: comparison of four assays for OH. Free Radic Biol Med 1987;3:33–39. [PubMed: 3040537]
27. Benesch RE, Lardy HA, Benesch R. The sulfhydryl groups of crystalline proteins. I. Some albumins, enzymes, and hemoglobins. J Biol Chem 1955;216:663–676. [PubMed: 13271343]
28. Kortemme T, Darby NJ, Creighton TE. Electrostatic interactions in the active site of the N-terminal thioredoxin-like domain of protein disulfide isomerase. Biochemistry 1996;35:14503–14511. [PubMed: 8931546]
29. Roberts BR, Wood ZA, Jönsson TJ, Poole LB, Karplus PA. Oxidized and synchrotron cleaved structures of the disulfide redox center in the N-terminal domain of *Salmonella typhimurium* AhpF. Protein Sci 2005;14:2414–2420. [PubMed: 16131664]
30. Lo Bello M, Parker MW, Desideri A, Polticelli F, Falconi M, Del Boccio G, Pennelli A, Federici G, Ricci G. Peculiar spectroscopic and kinetic properties of Cys-47 in human placental glutathione transferase. Evidence for an atypical thiolate ion pair near the active site. J Biol Chem 1993;268:19033–19038. [PubMed: 8360190]
31. Sarkany Z, Szeltner Z, Polgar L. Thiolate-imidazolium ion pair is not an obligatory catalytic entity of cysteine peptidases: the active site of picornain 3C. Biochemistry 2001;40:10601–10606. [PubMed: 11524003]
32. Jocelyn, PC. Biochemistry of the SH Group. Academic Press; New York: 1972.

33. Lindley H. A study of the kinetics of the reaction between thiol compounds and choloracetamide. Biochem J 1960;74:577–584. [PubMed: 14417169]
34. Nelson JW, Creighton TE. Reactivity and ionization of the active site cysteine residues of DsbA, a protein required for disulfide bond formation in vivo. Biochemistry 1994;33:5974–5983. [PubMed: 8180227]
35. Kallis GB, Holmgren A. Differential reactivity of the functional sulfhydryl groups of cysteine-32 and cysteine-35 present in the reduced form of thioredoxin from *Escherichia coli*. J Biol Chem 1980;255:10261–10265. [PubMed: 7000775]
36. Parsonage D, Karplus PA, Poole LB. Substrate specificity and redox potential of AhpC, a bacterial peroxiredoxin. Proc Natl Acad Sci U S A 2008;105:8209–8214. [PubMed: 18165315]
37. Poole LB, Higuchi M, Shimada M, Calzi ML, Kamio Y. *Streptococcus mutans* H_2O_2-forming NADH oxidase is an alkyl hydroperoxide reductase protein. Free Radic Biol Med 2000;28:108–120. [PubMed: 10656297]
38. Peskin AV, Low FM, Paton LN, Maghzal GJ, Hampton MB, Winterbourn CC. The high reactivity of peroxiredoxin 2 with H_2O_2 is not reflected in its reaction with other oxidants and thiol reagents. J Biol Chem 2007;282:11885–11892. [PubMed: 17329258]
39. Nordstrand K, Aslund F, Meunier S, Holmgren A, Otting G, Berndt KD. Direct NMR observation of the Cys-14 thiol proton of reduced *Escherichia coli* glutaredoxin-3 supports the presence of an active site thiol-thiolate hydrogen bond. FEBS Lett 1999;449:196–200. [PubMed: 10338131]
40. Mössner E, Huber-Wunderlich M, Glockshuber R. Characterization of *Escherichia coli* thioredoxin variants mimicking the active-sites of other thiol-disulfide oxidoreductases. Prot Sci 1998;7:1233–1244.
41. Karplus, PA.; Hall, A. Structural Survey of the Peroxiredoxins. In: Flohé, L.; Harris, JR., editors. Peroxiredoxin Systems. Springer; New York: 2007. p. 41-60.
42. Diederichs K, Karplus PA. Improved R-factors for diffraction data analysis in macromolecular crystallography. Nat Struct Biol 1997;4:269–275. [PubMed: 9095194]

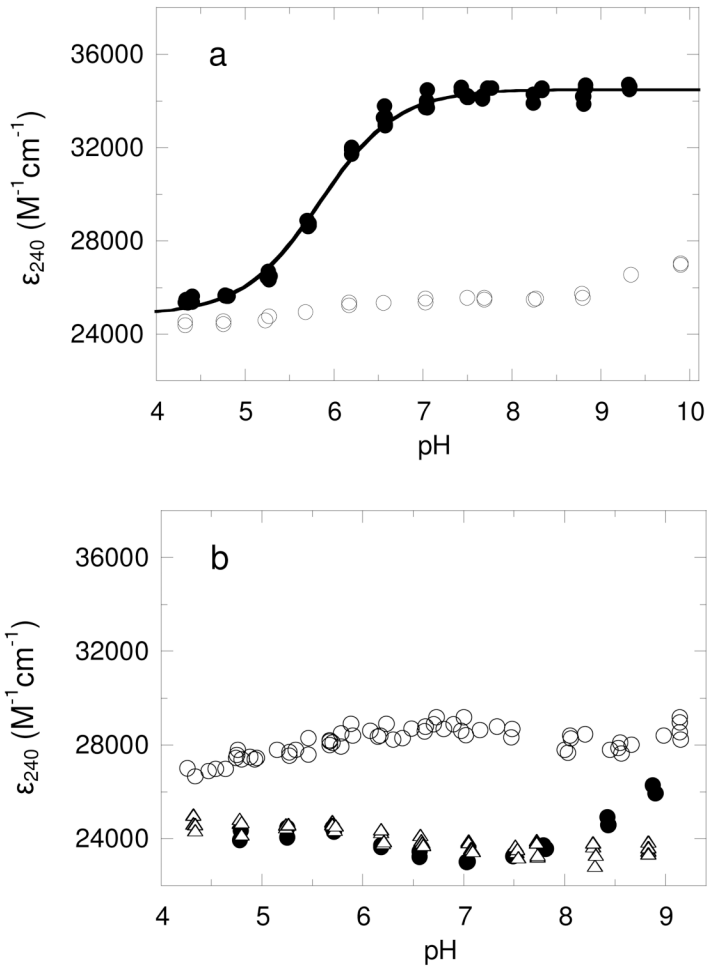

FIGURE 1. Monitoring cysteine thiolate absorption of wild type AhpC at 240 nm over a pH range yields a single pK_a value of 5.84 ± 0.02

(a) The A_{240} and A_{280} values for oxidized (o) and reduced (●) AhpC (3-10 μM) were measured over a range of pH values and converted to ε_{240} assuming an ε_{280} value of 24,300 M^{-1} cm^{-1}. The pK_a was determined from the ε_{240} versus pH plot by direct fit to Equation 1 as described in Methods. (b) As described for panel a, the pH-dependent change in absorbance was measured for C46S (o), C165S (●) and the C46S, C165S double mutant of AhpC (Δ). These data were not able to be fit to equation 1.

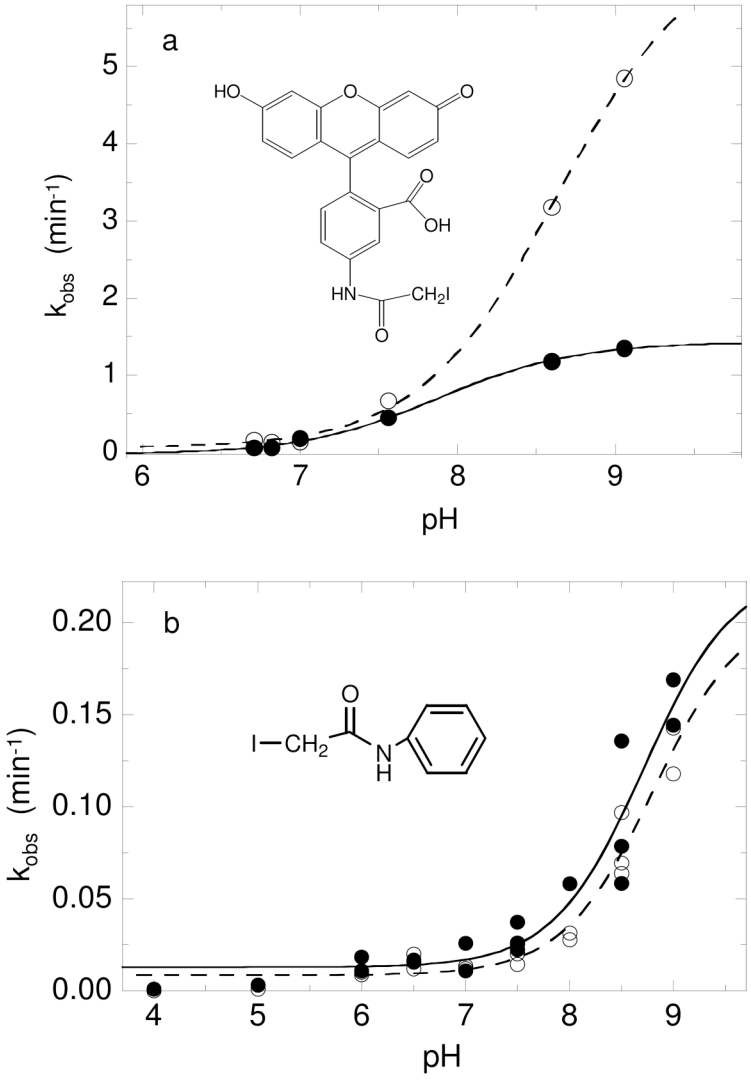

FIGURE 2.

pK_a determination using two different iodoacetamide-based compounds and single cysteine mutants of AhpC provide pK_a values for C46 and C165 close to 8.5. (a) Reduced C165S (—●—) or C46S (- -○- -) AhpC (24 μM) in various pH buffers was incubated with 180 μM 5-iodoacetamidofluorescein for various amounts of time, quenched with excess 2-mercaptoethanol, then analyzed on a 12% SDS-polyacrylamide gel to determine the % fluorescence in the protein fraction; the data were fit to a single exponential equation to determine k_{obs} at each pH. Data plotted as k_{obs} *versus* pH were fit to equation 1 as described in Methods. (b) Reduced wild-type AhpC (40 μM) in various pH buffers was incubated with 400 μM d_0-IAAn over a time course, and aliquots were quenched with excess 2-mercaptoethanol. A standard amount of AhpC labeled with d_5-IAAn was added to each sample, and the protein was digested with trypsin overnight as described in Experimental Procedures. The extent of alkylation of C46 (—●—) and C165 (- -○- -) was determined by measuring the ratio of the peak intensities at 3836/3841 or 1745/1750 Da, respectively. The ratios were fit to a single exponential equation to determine the k_{obs} and used to calculate the pK_a of each residue as in panel (a).

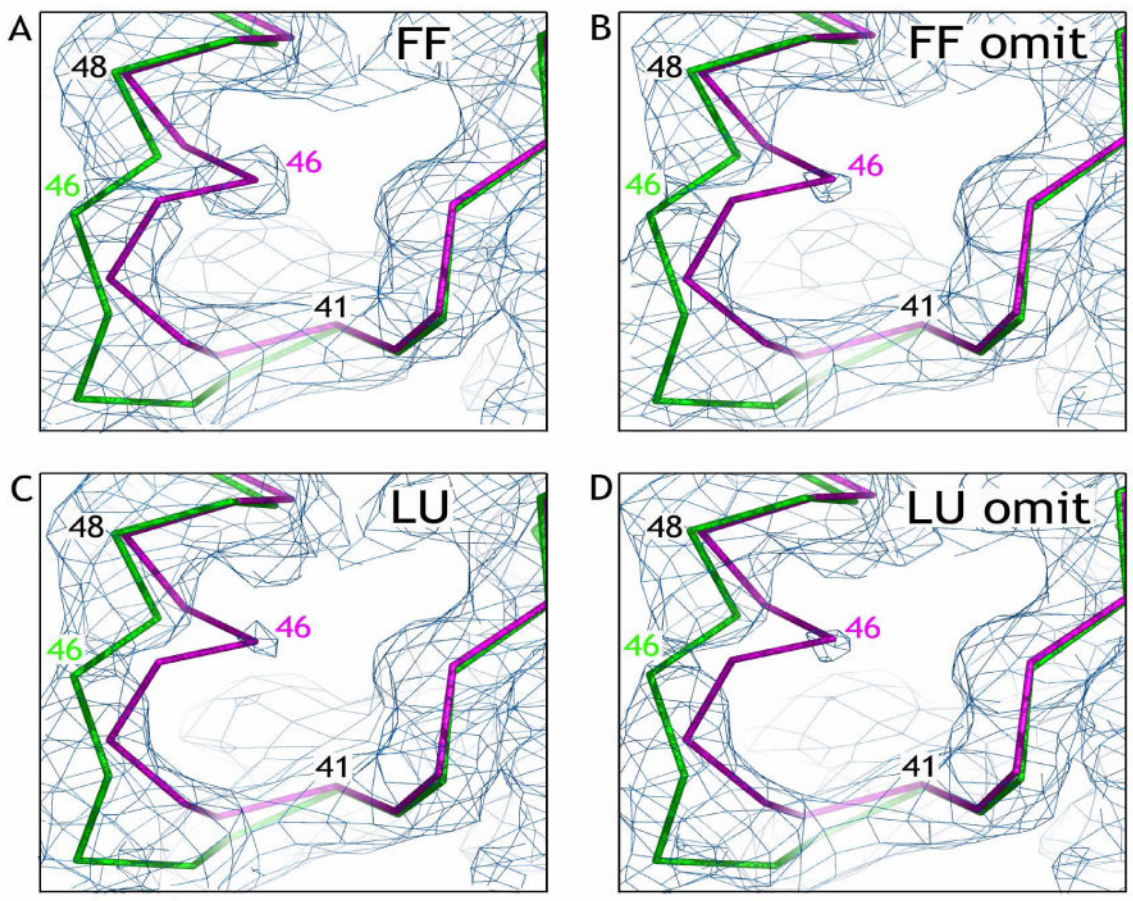

FIGURE 3.

Crystal structure of C165S AhpC adduct with iodoacetanilide shows that the protein is in the locally unfolded conformation. In each panel, the Cα chain of residues 38 through 50 from the fully folded (FF) model (magenta) and the locally unfolded (LU) model (green) are shown along with 2Fo-Fc electron density contoured at 0.7·ρrms. (a and c) Electron density calculated using the FF or LU model, respectively; (b and d) Electron density calculated using the FF or LU model, respectively, with residues 41 through 48 omitted. Figures were prepared using Pymol.

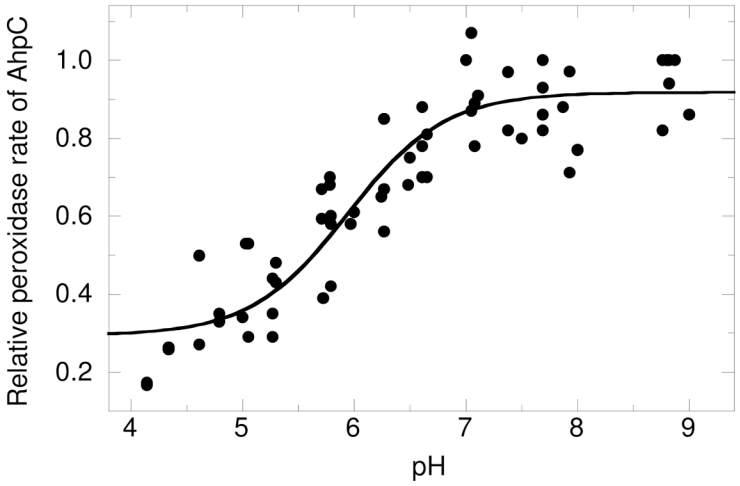

FIGURE 4. pK_a determination for wild type AhpC using a competition assay with horseradish peroxidase (HRP) yields a pK_a of 5.94 ± 0.10

Three μM H_2O_2 was added to HRP (7.5 μM) and reduced AhpC (0, 2, 4, 8, 12, or 16 μM) in various pH buffers. The extent of HRP oxidation by H_2O_2 was monitored using A_{403} (to measure complex I formation in HRP) before peroxide addition and again within 90 s after initiation of the reaction. The percentage of inhibition of HRP oxidation *(F/*1–*F) versus* [AhpC] was used to calculate the second-order rate constant for AhpC (k_{AhpC}) using equation 2 (see Methods and Supplemental Figures S2 a and b). Data plotted as either k_{AhpC} or relative rate *versus* pH were fit to equation 1 as described in Experimental Procedures.

Table 1

Data Collection and Refinement Statistics for C165S AhpC Alkylated With Iodoacetanilide (AhpC-C46AAn).

Data Collection[1]	
Resolution (Å)	100 - 4.0 (4.14 – 4.0)
No. of unique observations	13503
Multiplicity	8.8 (8.9)
Completeness (%)	98.4
I/σ	12.2 (5.3)
Mosacity	0.87
R_{meas}[2] (%)	14.3 (51.9)
R_{mrdg-F}[2] (%)	12.7 (38.5)
Refinement	
Fully-Folded R_{factor} / R_{free}	0.366 / 0.371
Locally Unfolded R_{factor} / R_{free}	0.378 / 0.390[3]

[1] Numbers in parentheses correspond to the highest resolution bin.

[2] R_{meas} is the multiplicity weighted merging R-factor and R_{mrgd-F} is an indicator of the quality of reduced data (42).

[3] Final rigid body refinement of the locally unfolded model after manual rebuilding to minimize clases gives an R_{factor} / R_{free} of 0.301/0.308.

Table 2

Reaction Rates of *St*AhpC With Various Iodoacetamide Derivatives and Hydroperoxides at pH7.

	Reaction rate with AhpC (min^{-1})[a]
Fluorescein iodoacetamide	0.67
Iodoacetanilide	0.031
Iodoacetamide	0.0035
Hydrogen peroxide	3130[b]
Cumene hydroperoxide	2460[b]

[a] Prereduced AhpC (40 μM) was incubated in pH 7 buffer with 400 μM iodoacetamide, iodoacetanilide (IAAn), or fluorescein iodoacetamide. Rates of reaction with iodoacetamide and IAAn were determined by a subsequent thiol assay conducted at multiple time points, whereas modification by fluorescein iodoacetamide was assessed using a gel method to detect fluorescently-labeled protein as described in Methods.

[b] The reaction rates of AhpC with hydrogen peroxide and cumene hydroperoxide were calculated from the previously determined steady state parameters, k_{cat} and K_m (1,36).